Journal of the European Ceramic Society 15 (1995) 1119–1124

0955-2219(95)00093-3
0955-2219/95/$9.50

Crystallization of Metastable Tetragonal Zirconia from the Decomposition of a Zirconium Alkoxide Derivative

David E. Collins, Kirk A. Rogers & Keith J. Bowman*

School of Materials Engineering, Purdue University, West Lafayette, IN 47907, USA

(Received 24 February 1995; revised version received 19 May 1995; accepted 22 May 1995)

Abstract

A zirconium alkoxide derivative, dibutoxybis(acetylacetonato) zirconium, was polymerized at 120°C and 300 millitorr for 3 h to form oligomers, as characterized by gel permeation chromatography and Fourier transform infra-red spectroscopy. Pyrolysis of the precursor at 675°C in flowing 5% H_2 in N_2 followed by cooling to room temperature, produced nano-scale, tetragonal ZrO_2 considerably below the tetragonal-to-monoclinic transformation temperature (approximately 1200°C). Subsequent heat treatment of the same precursor in flowing air under otherwise identical conditions produced approximately 8 vol% monoclinic ZrO_2. The possible formation of oxygen vacancies from polymer pyrolysis and their role in nucleating the metastable tetragonal phase are discussed.

1 Introduction

It has been well documented[1–4] that the pyrolysis of zirconium-based precursors produces a metastable tetragonal phase below the monoclinic–tetragonal transition temperature (approximately 1200°C) with crystallite sizes reported in the range of 5 to 460 Å.[2,3] Several investigators,[5–7] including Livage *et al.*[1] and Clearfield,[8] have speculated that the metastability of tetragonal zirconia (t-ZrO_2) is attributed to the structural similarities between the precursor phase and the tetragonal phase. In conjunction with these structural similarities, Livage *et al.*[1] and Osendi *et al.*[3] discussed the nonstoichiometry associated with the metastable tetragonal phase. By crystallizing ZrO_2 from zirconyl chloride *in vacuo*, Livage *et al.*[1] showed that a nonstoichiometric tetragonal phase predominated, whereas crystallization in air produced the monoclinic phase. From electron paramagnetic resonance studies on ZrO_2 crystallized from zirconyl chloride, Osendi *et al.*[3] concluded that tetragonal metastability results from lattice defects, specifically anionic vacancies, created upon crystallization. More recently, Igawa *et al.*[9] refined crystal structure calculations for the metastable tetragonal phase using neutron diffraction and Rietveld analysis on ZrO_2 crystallized from $Zr(O(CH_2)_3CH_3)_4$. They concluded that the crystal lattice coincided with those of doped tetragonal structures rather than pure t-ZrO_2 at 1200°C. However, in all of these cases, the origin of nonstoichiometry is unclear.

In spite of this ambiguity, these conclusions suggest that ZrO_2 crystal structure might be tailored by the choice of precursor and processing. An appealing application would be the formation of t-ZrO_2 with a preferred orientation caused by the processing of oriented, zirconium-based polymers. For such a processing strategy to be successful, the molecular configuration of the polymer must influence the final crystal structure. Establishing the existence of such a relationship relies on a full understanding of the precursor-to-ceramic transition. However, what factors influence structure on the molecular level during pyrolysis remain a critical issue not resolved in the literature. Although our intent is to control zirconia crystallization, the underlying goal is to address metallo-organic decomposition from a molecular standpoint. In this paper, we describe a mechanism by which the molecular configuration of a zirconium-based polymer might influence structural features in the pyrolysis product.

2 Experimental Procedure

Dibutoxybis(acetylacetonato) zirconium (BAZ), represented as:

*To whom correspondence should be addressed.

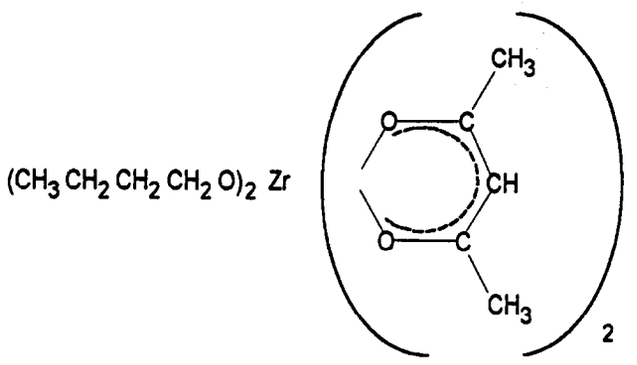

was obtained in a 60 wt% solution of n-butanol (97% pure 2:1 (alkoxide-to-zirconium); the remaining 3% is 1:1) from Gelest Inc., Tullytown, PA, USA. The excess n-butanol was distilled from the solution *in vacuo*, resulting in a yellow oil. Similar to the method described by Yogo,[10] the remaining BAZ was refluxed for 3 h at 120°C and 300 millitorr such that a reddish-brown gel was formed upon cooling to room temperature. To remove the retained solvent, samples were dried in flowing 5% H_2 in N_2 (300 cm^3 min^{-1}) at 200°C for 12 h, producing a fine orange powder. Samples were then fired at 675°C in a flowing gas, either H_2 in N_2 or air (300 cm^3 min^{-1}), and then allowed to cool to room temperature.

Fourier transform infra-red spectroscopy (FTIR), performed on a Nicolet 550 infra-red spectrometer, was used to identify structural features of the polymerized complex. The analysis was restricted to vibrational energies in the mid-infra-red spectrum, corresponding to a wavenumber range of 4000–400 cm^{-1}. For this study, neat samples were prepared by dispersing ground samples onto NaCl plates. Gel permeation chromatography (GPC), by Lark Enterprises, Webster, MA, USA, was used to determine the relative molecular weight and shape of the polymerized complex in solution as compared with a polystyrene standard. Styragel HR 2, 1, and 0·5 columns, employed for the analysis, were operated at 37°C using tetrahydrofuran as the mobile phase. A low molecular weight oligomer mix of polystyrene was used as a standard for calibration. Transmission electron microscopy (TEM) samples were prepared by grinding the samples with a mortar and pestle into a powder that could be applied to a graphite-coated Cu grid using acetone as the carrying medium. A JEOL 2000 FX operated at 200 kV was used to conduct bright-field imaging and selected-area diffraction (SAD) studies.

X-ray diffraction (XRD) performed on a Siemens D500 diffractometer with CuKα radiation was used to determine the phases present and the crystallite size using the Scherrer equation with respect to the {1 1 1} reflections.[11] The monoclinic volume fraction, v_m, was calculated from the linear intensity relationship

$$v_m = \frac{I_m(\bar{1}\,1\,1) + I_m(1\,1\,1)}{I_m(\bar{1}\,1\,1) + I_m(1\,1\,1) + I_t(1\,1\,1)} \quad (1)$$

where the subscripts m and t represent monoclinic and tetragonal, respectively. Although eqn (1) is consistent with literature on this topic, several investigators[12–14] have demonstrated that v_m calculated from eqn (1) can deviate from the actual v_m as much as 20% at $v_m = 0{\cdot}46$. Modifications based on structure factor calculations have been suggested,[12] unfortunately, an accurate diffraction model for metastable ZrO_2 that addresses stoichiometry and corresponding ionic position remains to be developed.

3 Results and Discussion

3.1 Molecular structure

The FTIR spectra in Fig. 1 impart information regarding the molecular structure and the precursor-to-ceramic transition of this organozirconium complex. The peak assignments were made by comparison to similar metal alkoxides[15,16] and metal bisacetylacetonate complexes.[17–19] Table 1 lists the observed frequencies and band assignments for this zirconium complex.

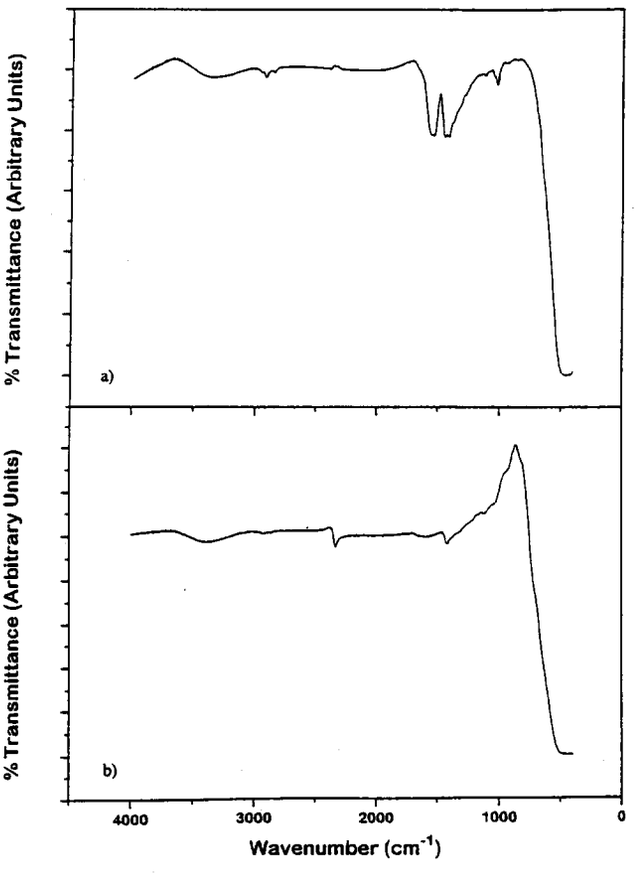

Fig. 1. Fourier transform infra-red (FTIR) spectra of (a) dried sample and (b) sample pyrolysed at 675°C.

Table 1. Observed frequencies and band assignments of *cis*-oligo[dibutoxybis(acetylacetonato) zirconium] (COBAZ) dried at 200°C; ν denotes stretching frequencies, δ denotes deformation frequencies

Observed frequencies (cm^{-1})	*Band Assignments*
3350	ν –OH
2920	ν –CH
2850	ν –CH
1550	ν C = O
1453	δ $-CH_3$
1420	δ –CH
1120	ν C – O
1025	ν Zr = O
452	ν Zr – O – Zr

The residual–OH bands in the spectra of the dried sample (Fig. 1(a)) result from possible hydrolysis of butoxy groups. The absence of bands ascribed to acetylacetonate (acac), such as Zr =O and $-CH_3$, in the spectra taken of the pyrolysed sample at 675°C in air (Fig. 1(b)) signify bidentate ligand decomposition during the pyrolysis process, leaving only the Zr–O–Zr bonds. These oxo bonds are consistent with investigations by Barraclough *et al.*[15] and Bradley *et al.*[20] which have shown that zirconium atoms, similar to other metal atoms, can be electrostatically bonded as follows:

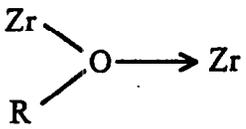

where R represents $CH_3(CH_2)_3$ in this case.

Figure 2 shows the resulting GPC chromatograph of the precursor. The broad peak corresponds to a wide range of molecules having similar molecular weights, whereas the distinct peaks correspond to large concentrations of specific low molecular weight molecules. Preliminary GPC data indicated that the precursor molecular weight was less than the monomer

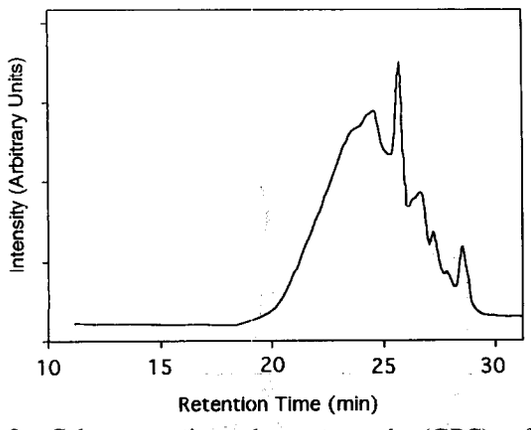

Fig. 2. Gel permeation chromatograph (GPC) of *cis*-oligo[dibutoxybis(acetylacetonato) zirconium] (COBAZ) in tetrahydrofuran.

Table 2. The molecular weight and average degree of polymerization as determined by gel permeation chromatography (GPC)

Retention time (min)	*Molecular weight (g mol^{-1})*	*Degree of polymerization*	*Average degree of polymerization*
29·15	335·99	0·77	
28·65	434·91	1·00	0·98
28·35	507·75	1·17	
27·60	747·76	1·72	
27·50	787·36	1·81	1·91
27·12	957·97	2·20	
27·00	1019·18	2·34	
26·80	1130·00	2·60	2·90
26·08	1638·58	3·77	
26·04	1672·80	3·85	
25·80	1893·35	4·35	4·24
25·72	1973·16	4·54	
25·23	2540·95	5·84	
24·68	3375·03	7·76	19·52
24·38	3940·24	9·06	
24·10	4552·87	10·47	
23·53	6110·13	14·05	
20·42	30419·85	69·93	

molecular weight, suggesting that the precursor was retained in the column more readily than the polystyrene standard; possibly due to apparent molecular size or packing interactions. From this observation, the molecular weight distribution was normalized to the last eluted peak, corresponding to the monomer molecular weight. Table 2 lists the molecular weight ranges assigned to the remaining peaks. Once normalized, the values of the adjacent peaks 2, 3 and 4 correspond to a dimer, trimer and tetramer, respectively.

The molecular architecture of these oligomers depends on the *cis*- or *trans*-configuration of the monomer as shown by Bradley and Holloway in an analogous system.[21,22] In their study, proton nuclear magnetic resonance (H^1 NMR) analysis of titanium bisacetylacetonate derivatives $(Ti(acac)_2(OR)_2$ where R represents Me, Et, Pr^i, Bu^t groups, etc.) demonstrated that the *cis*-isomer is favoured over the *trans*-isomer. Following this premise, the *cis*-monomers combine by alkoxy bridges, as described by Thomas,[23] forming oligomers during polymerization. The resulting oligomers, *cis*-oligo[dibutoxybis(acetylacetonato) zirconium] (COBAZ), have a host of structural isomers dependent on this *cis*-configuration and steric factors associated with the organic ligands. Two possible structures, a 'linear' and a cyclic configuration, of a tetrameric oligomer are depicted schematically in Fig. 3. For clarity, the $CH_3(CH_2)_3$ groups bonded to the oxygens that bridge the zirconiums together have been left off. Within the COBAZ backbone, each zirconium has an eight-fold coordination with oxygen; however, each zirconium in

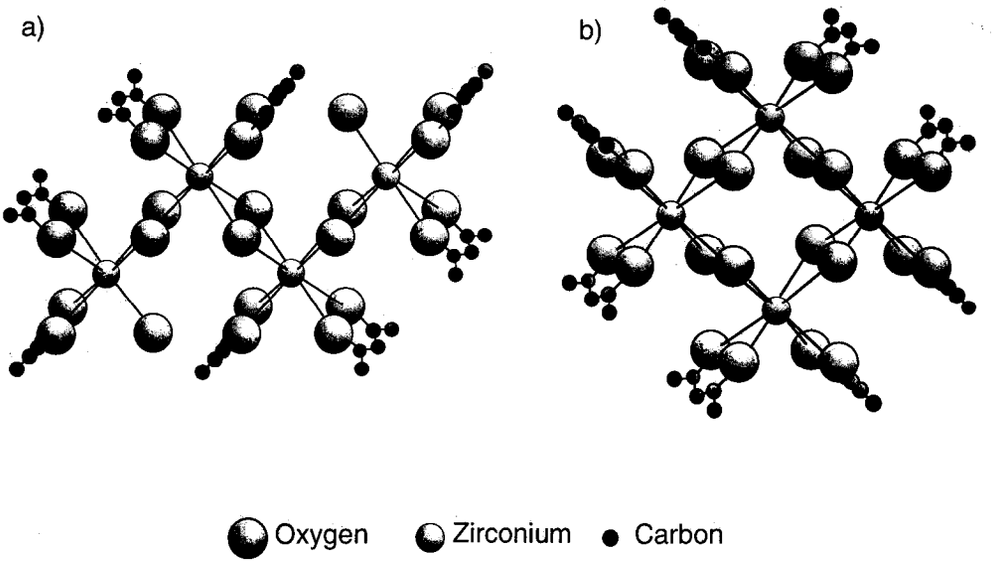

Fig. 3. Molecular structures of (a) 'linear' and (b) cyclic tetrameric *cis*-oligo[dibutoxybis(acetylacetonato) zirconium] (COBAZ). Hydrogen atoms and alkyl groups have been omitted for clarity.

the terminal positions has a seven-fold coordination due to an unshared alkoxy ligand not used in bridging, see Fig. 3(a). The acetylacetonate ligands, which hinder reaction due to steric obstruction during the polymerization process,[24] form the perimeter of the oligomer.

3.2 Pyrolysis

Although the COBAZ XRD data do not demonstrate any long-range order, brightfield imaging and SAD in TEM show (see Fig. 4) COBAZ to comprise nano-scale crystallites. Pyrolysing these COBAZ crystallites under reducing conditions of flowing 5% H_2 in N_2 produces a completely tetragonal oxide (see Fig. 5(a)), black from incomplete combustion of the organic material. The average crystallite size, approximately 110 Å, falls within such a range that line broadening masks resolution of the {200}, {220} and {113} peaks. The same sample annealed in flowing air under otherwise identical conditions shows the emergence of the (1 1 1) and ($\bar{1}$ 1 1) peaks of the monoclinic phase as can be seen in Fig. 5(b). XRD data indicate that

Fig. 4. Transmission electron micrograph (TEM) and selected-area diffraction (SAD) data of the dried precursor.

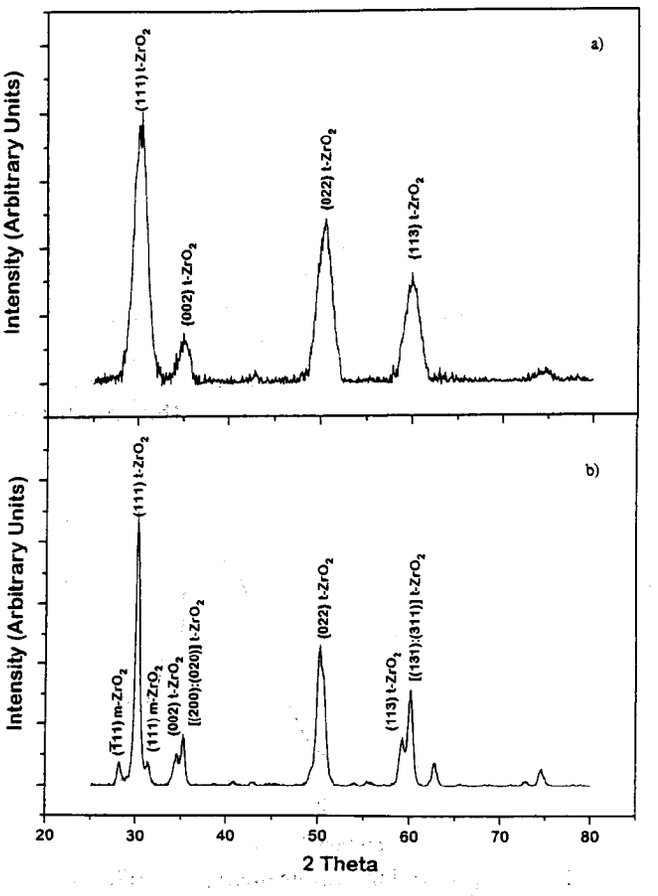

Fig. 5. X-ray diffraction (XRD) data of sample pyrolysed at 675°C in (a) flowing 5% H_2 in N_2 and (b) flowing air.

after 12 h of exposure to oxygen in air, 8 vol% of the tetragonal phase with an average crystallite size of approximately 480 Å underwent a phase transformation to m-ZrO_2 with a crystallite size of 570 Å. Furthermore, the resulting white powder was more friable after exposure to oxygen, indicative that the transformation had occurred.

Interpretation of this outcome can be related to significant structural features on the molecular level. Analogous to zirconyl chloride, COBAZ has a similar molecular structure to the t-ZrO_2 crystal lattice with the exception of the terminal positions. Upon heat treatment, the organic material decomposes, allowing the alkoxy bridges to undergo oxolation, the process by which the alkoxy bridges convert to oxygen bridges. At this point, the eight-fold coordination of zirconium within the oligomeric chain is retained, which is also true of the seven-fold coordination of the terminal zirconium. Upon pyrolysis, the terminal positions become likely sites for lattice defects, more specifically oxygen vacancies. We propose that these defects retained from the COBAZ structure are instrumental in producing the tetragonal phase during nucleation of the ZrO_2 crystallites under oxygen-deficient conditions. A similar phenomenon has been documented for other martensite systems in which point defects sustain tetragonality.[25] This inception of lattice defects based on the initial structure of the precursor may also explain the nonstoichiometry that Livage *et al.*[1] and Osendi *et al.*[3] saw in their investigations.

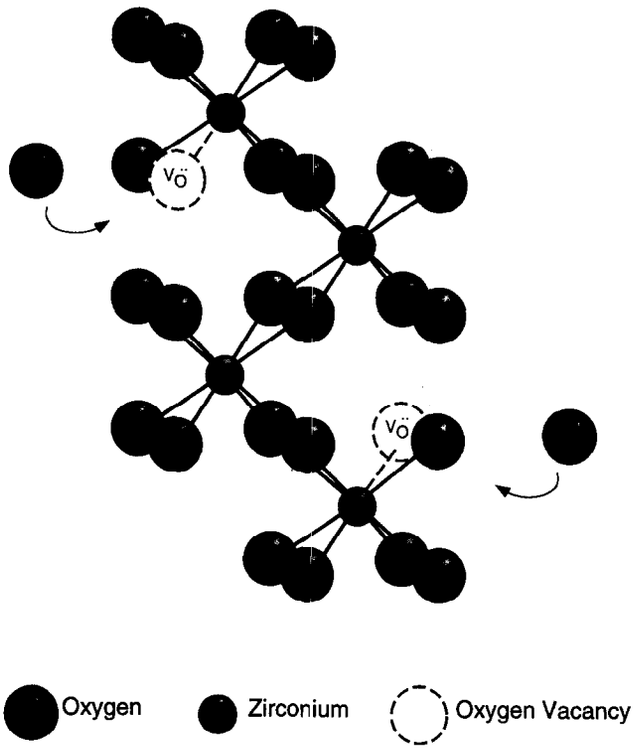

Fig. 6. Schematic of oxygen movement into oxygen vacancies that act as dopants to stabilize the tetragonal phase of zirconia during crystallization of a zirconium-based polymer. The polymer is at a point in pyrolysis in which the organic material has decomposed.

Akin to the work of Igawa *et al.*,[9] the resulting nano-crystallite, metastable t-ZrO_{2-x} should have lattice parameters similar to those of doped zirconias at room temperature. The probability of transformation to the monoclinic phase during this onset of nucleation may be relatively small due to the crystallite size.[26] Upon further heat treatment in the presence of oxygen, the anionic vacancies fill as depicted in Fig. 6. A sufficient decrease in the number of these vacancies should facilitate instability in the metastable tetragonal phase. Our results also show that crystallite coarsening and residual carbon accompany the pyrolysis. Because the metastable phenomenon also occurs in the zirconyl chloride system which is devoid of residual carbon, its actual influence is questionable; however, evidence that carbon may stabilize nonstoichiometry has been found in the literature and cannot be ignored.[27] Unfortunately, assessing the role that these factors play in nucleation, transformation and stability of metastable, tetragonal crystallites is not easily accomplished.

4 Summary

To address metallo-organic decomposition on the molecular level, we have found that the molecular configuration of the precursor, COBAZ, and the resulting oxide after pyrolysis are intimately related. We propose that zirconium, within the COBAZ backbone, has an eight-fold coordination to oxygen, similar to the t-ZrO_2 unit cell; whereas terminal zirconium has a seven-fold coordination. When pyrolysed in the absence of oxygen, COBAZ nucleates a completely t-ZrO_{2-x} bearing oxygen vacancies retained from the COBAZ structure, particularly from the terminal zirconium positions. These vacancies play an integral role in tetragonal nucleation. When t-ZrO_{2-x} is heat treated in the presence of oxygen under otherwise identical conditions, a fractional amount of monoclinic phase develops. This introduction of oxygen diminishes the number of vacancies such that tetragonal instability occurs, facilitating monoclinic growth.

Acknowledgments

We would like to thank H. Lackritz, K. Trumble and E. Slamovich for their insightful contributions to this investigation. This research was supported by The National Science Foundation DMR-91-21948.

References

1. Livage, J., Doi, K. & Mazieres, C., Nature and thermal evolution of amorphous hydrated zirconium oxide. *J. Am. Ceram. Soc.*, **51**(6) (1968) 349–53.
2. Mitsuhashi, T., Ichihara, M. & Tatsuke, U., Characterization and stabilization of metastable tetragonal ZrO_2. *J. Am. Ceram. Soc.*, **57**(2) (1974) 97–101.
3. Osendi, M., Moya, J., Serna, C. & Soria, J., Metastability of tetragonal zirconia powders. *J. Am. Ceram. Soc.*, **68**(3) (1985) 135–9.
4. Tani, E., Yoshimura, M. & Somiya, S., Formation of ultrafine tetragonal ZrO_2 powder under hydrothermal conditions. *J. Am. Ceram. Soc.*, **66** (1983) 11–14.
5. Fryer, J., Hutchison, J. & Paterson, R., An Electron microscopic study of the hydrolysis products of zirconyl chloride. *J. Colloid Interface Sci.*, **34**(2) (1970) 238–48.
6. Mamott, G., Barnes, P., Tarling, S., Jones, S. & Norman, C., Dynamic studies of zirconia crystallization. *J. Mater. Sci.*, **26** (1991) 4054–61.
7. Turrillas, X., Barnes, P., Tarling, S., Jones, S., Norman, C. & Ritter, C., Neutron thermodiffractometry and synchrotron energy-disperive diffraction studies of zirconium hydroxide calcination. *J. Mater. Sci. Let.*, **12** (1993) 223–6.
8. Clearfield, A., Structural aspects of zirconium chemistry. *Rev. Pure Appl. Chem.*, **14** (1964) 91–108.
9. Igawa, N., Ishii, Y., Nagasaki, T., Morii, Y., Funahashi, S. & Ohno, H., Crystal structure of metastable tetragonal zirconia by neutron powder diffraction study. *J. Am. Ceram. Soc.*, **76**(10) (1993) 2673–6.
10. Yogo, T., Synthesis of polycrystalline zirconia fiber with organozirconium precursor. *J. Mater. Sci.*, **25** (1990) 2394–8.
11. Klug, H. & Alexander, L., *X-Ray Diffraction Procedures.* John Wiley & Sons Inc., New York, 1954.
12. Toraya, H., Yoshimura, M. & Somiya, S., Quantitative analysis of monoclinic-stabilized cubic ZrO_2 systems by X-ray diffraction. *J. Am. Ceram. Soc.*, **67**(6) C183–121.
13. Evans, P., Stevens, R. & Binner, J., Quantitative X-ray diffraction anaylsis of polymorphic mixes of pure zirconia. *Br. Ceram. Trans. J.*, **83**(2) (1984) 39–43.
14. Schmid, H., Quantitative analysis of polymorphic mixes of zirconia by X-ray diffraction. *J. Am. Ceram. Soc.*, **70**(5) (1987) 367–76.
15. Barraclough, C., Bradley, D., Lewis, J. & Thomas, I., The infrared spectra of some metal alkoxides, trialkylsilyloxides, and related silanols. *J. Chem. Soc.*, (1961) 2601.
16. Lynch, C., Mazdiyasni, K., Smith, J. & Crawford, W., Infrared spectra of transition metal alkoxides. *Anal. Chem.*, **36** (1964) 2332.
17. Mikami, M., Nakagawa, I. & Shimanouchi, T., Far infra-red spectra and metal–ligand force constants of acetylacetonates of transition metals. *Spectrochim. Acta*, **23A** (1967) 1037.
18. Nakamoto, K., *Infrared Spectra of Inorganic and Coordination Compounds.* John Wiley & Sons, Inc., New York, 1970.
19. Barraclough, C., Lewis, J. & Nyholm, R., The stretching frequencies of metal–oxygen double bonds. *J. Chem. Soc.*, (1959) 3552.
20. Bradley, D., Mehrotra, R., Swanwick, J. & Wardlaw, W., Structural chemistry of the alkoxides. Part IV. Normal alkoxides of silicon, titanium, and zirconium. *J. Chem. Soc.*, (1953) 2025–30.
21. Bradley, D. & Holloway, C., Some Labile cis-dialkoxybis (aceylacetonato) titanium (IV) compounds. *Chem. Commun.*, (1965) 284.
22. Bradley, D. & Holloway, C., Nuclear magnetic resonance and infrared spectral studies on labile cis-dialkoxy-bis (acetylacetonato) titanium (IV) Compounds. *J. Chem. Soc. (A)*, (1969) 282.
23. Thomas, A., *Colloid Chemistry* McGraw-Hill Book Co., Inc., New York, 1934.
24. Papet, P., Le Gars, N., Baumard, J., Lecomte, A. & Dauger, A., Trasparent monolithic zirconia gels: effects of acetylacetone content on gelation. *J. Mater. Sci.*, **24** (1989) 3850–4.
25. Winchell, P. & Speich, G., Point-defect-supported martensite tetragonality. *Acta Met.*, **18** (1970) 53–62.
26. Garvie, R., The occurrence of metastable tetragonal zirconia as a crystallite size effect. *J. Phys. Chem.*, **69**(4) (1965) 1238–43.
27. Ackermann, R., Garg, S. & Rauh, E., High-temperature phase diagram for the system Zr–O. *J. Am. Ceram. Soc.*, **60** (7–8) (1977) 341–5.